P3.12 DRIZZLE IN STRATOCUMULUS CLOUDS: OBSERVATIONS AND MODEL RESULTS

Robert Wood*
The Met Office, Bracknell, Berkshire, United Kingdom

1. INTRODUCTION

The importance of drizzle to boundary layer clouds is unknown at present. It is therefore of some importance to obtain detailed observations of thermodynamic, dynamic, microphysical and structural characteristics of drizzling stratocumulus clouds in order to (i) elucidate controlling mechanisms and (ii) test and improve models of the drizzle process.

Due to the brevity of this paper I can only present a few examples of some of the characteristics of drizzling stratocumuli that are accessible in the dataset. The dataset consists of 12 flights (11 around the UK and 1 ASTEX flight). All observations were taken in relatively unbroken stratocumulus with mean cloud base precipitation rates ranging from 0.05 to 1.1 mm day^{-1}. Mean liquid water paths range from 45 to 360 g m^{-2}; mean droplet concentrations from 8-420 cm^{-3}. Tables 1 and 2 give additional details of the clouds sampled.

Table 1: Flight numbers, dates, locations, times, cloud type, mean heights of cloud base $\overline{z_{CB}}$ and cloud top ($\overline{z_i}$), mean liquid water path $\overline{LWP}$ (± error), mean in-cloud droplet concentration N_* and mean cloud base precipitation rate P_{CB}. Note that the errors are errors in the mean value and not estimates of the variability in that parameter.

Flight	Date	Location	Time [local]	Type	$\overline{z_{CB}}$ [m]	$\overline{z_i}$ [m]	$\overline{LWP}$ [g m^{-2}]	N_* [cm^{-3}]	P_{CB} [mm d^{-1}]
A049	6 Dec 90	SW App.	12-15	Sc	825±23	1450±34	260±44	310	0.49
A209	12 Jun 92	Azores	00-04	Sc	310±44	705±27	170±34	120	0.47
A439	29 Feb 96	NW Ireland	12-15	Sc	780±19	1150±9	100±15	90	0.24
A641	3 Dec 98	S. North Sea	11-16	Sc	430±7	1110±14	360±16	420	0.054
A644	14 Dec 98	SW App.	12-15	St	150±75	1800[1]	90±50	20	0.66
A648	28 Jan 99	SW App.	12-15	St	190±18	1550[1]	85±50	8	1.12
A649	29 Jan 99	SW App.	12-16	Sc	450±9	775±13	80±6	60	0.095
A693	8 Jul 99	NW Ireland	12-16	St/Sc	115±21	395±3	80±3	110	0.41
A762	12 Jun 00	SW App.	12-16	St/Sc	180±13	495±11	80±5	95	0.28
A763	14 Jun 00	SW App.	12-16	St/Sc	245±18	485±14	45±2	85	0.34
A764	15 Jun 00	SW App.	12-16	St/Sc	≈20	320±6	70±6	65	0.44
A767	28 Jun 00	North Sea	12-15	Sc w/Cu	935±24	1350±10	90±10	110	0.78

Note: 1. Multi-layered. Uppermost cloud top given.

2. VERTICAL STRUCTURE

A combination of straight and level runs and numerous sawtooth runs through the cloud layer was used to probe the cloud vertical structure with good resolution and sampling. Profiles of important parameters were generated as a function of the normalised height $z_* = (z - \overline{z_{CB}})/(\overline{z_i} - \overline{z_{CB}})$, where $\overline{z_{CB}}$ is the mean cloud base height and $\overline{z_i}$ is the mean cloud top (inversion) height. Figure 1 shows temperature (relative to the moist adiabatic temperature T_{moist} defined at the base of the cloud) and total water (relative to the mean value for the cloud layer q_{T*}) profiles in cloud for the 12 cases. The cases shown with lines are the relatively well mixed cases. The other two flights are from highly heterogeneous, somewhat stable multi-layered stratocumulus clouds that formed quite near to midlatitude frontal systems. For the well-mixed cases the moisture profiles are quite close to adiabatic and the temperature profiles tend to be slightly conditionally stable.

Table 1: In-cloud mean drizzle drop concentration $\overline{N_{d,D}}$, liquid water content $\overline{q_{L,D}}$ and precipitation rate $\overline{P}$. Also given are cloud top ($0.8 < z_* < 1.0$) and cloud base ($0.0 < z_* < 0.2$) values of the drizzle drop volume radius $r_{v,D}$

Case	$\overline{N_{d,D}}$ [l^{-1}]	$\overline{q_{L,D}}$ [10^{-3} g m^{-3}]	$\overline{P}$ [mm day^{-1}]	$r_{v,D}$ (base) [μm]	$r_{v,D}$ (top) [μm]
A049	37	11.3	0.51	53	38
A209	60	11.2	0.39	46	29
A439	30	7.5	0.26	45	35
A641	18	2.2	0.08	31	29
A644	59	20.9	0.99	42	43
A648	147	30.9	0.80	53	32
A649	46	6.8	0.17	38	30
A693	135	17.6	0.32	37	28
A762	170	17.7	0.28	36	26
A763	118	15.3	0.27	39	27
A764	89	21.8	0.58	44	35
A767	141	21.0	0.67	53	25

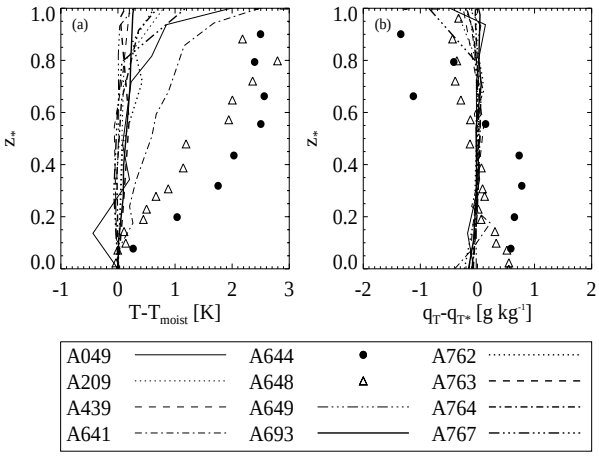

Figure 1: (a) Temperature and (b) total water content in-cloud profiles for each of the cases. Symbols are (a) the difference between the observed mean temperature at each height and the moist adiabatic temperature. (b) the difference between the mean total water content at each height and the mean total water content averaged over the entire cloud layer is plotted.

Figure 2 shows profiles of the mean and coefficient of

* *Corresponding author address*: Robert Wood, Atmospheric Sciences, University of Washington, Seattle, WA; *e-mail: robwood@atmos.washington.edu.*

variance (standard deviation/mean at that level) in cloud droplet concentration N_d and cloud liquid water content q_L. For the means droplet concentrations are normalised with the flight in-cloud mean N_* ; liquid water content is plotted as in Nicholls and Leighton (1986), i.e. as a departure from adiabatic LWC q_{ad} normalised with the adiabatic cloud top LWC. As in Nicholls and Leighton, most of the cases show somewhat subadiabatic liquid water content. Droplet concentrations are remarkably height-invariant away from the boundaries. The coefficient of variance in both droplet concentration and liquid water content is in the range 0.1-0.5 in the cloud centres and increases towards the cloud boundaries because of mesoscale variability in these boundaries (i.e. we include clear and cloudy air in the layer means and variances). Cloud fraction (not shown) in the well mixed cases increases from 0.4-0.7 at mean cloud base to unity at $z_* = 0.2 - 0.3$, and decreases again at $z_* > 0.7 - 0.8$.

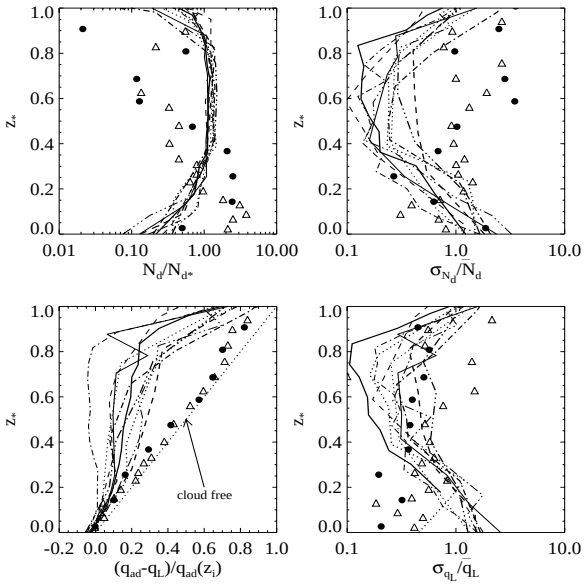

Figure 2: Profiles of (a) droplet concentration N_d, (b) standard deviation of droplet concentration at each level normalised with the mean at each level; (c) values of the subadiabaticity parameter $(q_{ad} - q_L)/q_{ad}(z_i)$ for which zero represents a perfectly adiabatic cloud. The dotted line represents cloud free conditions; (d) the standard deviation of the liquid water content normalised with the mean at that level. Symbolia are the same as for Fig. 1.

Figure 3 shows profiles of mean drizzle drop concentration (radius$> 20\mu$m), mean volume radius of drizzle drops, drizzle LWC and precipitation rate for the cases. There is a reasonably tight bunching of the well-mixed cases for (a), (c) and (d). The drizzle droplet concentration tends to increase slightly with height (taking into account the cloud fraction). The volume radius of drizzle drops increases downwards in cloud due to the coalescence and sedimentation process (see Table 2). Drizzle liquid water content $q_{L,D}$ is relatively constant with height in the body of the cloud. Precipitation rates P tend to increase downwards in cloud.

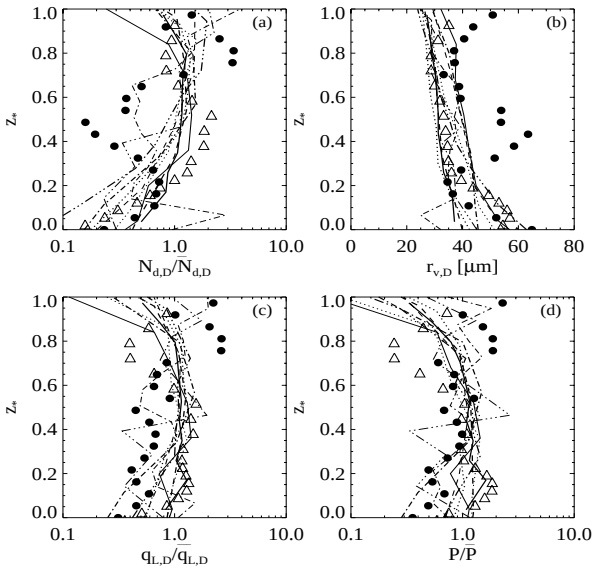

Figure 3: Profiles of characteristics relating to the drizzle drops, which are defined here as drops with radii larger than 20 μm. (a) Drizzle droplet concentration $N_{d,D}$ normalised with the mean drizzle droplet concentration in the cloud layer; (b) volume radius of drizzle drops $r_{v,D}$ which increases towards cloud base; (c) liquid water content contained in the drizzle drops normalised with the mean value for the cloud layer; (d) precipitation rate normalised with the mean value in the cloud layer. Symbols are as Fig. 1.

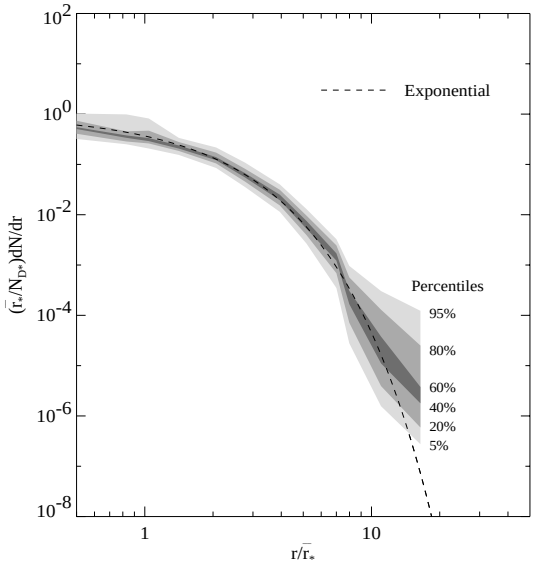

Figure 4: Normalised droplet spectra $(\overline{r_*}/N_{D*})dN/dr$ at all in-cloud levels (103 spectra) plotted against $r/\overline{r_*}$. The universal exponential distribution $(\overline{r_*}/N_{D*})dN/dr = \exp(-r/\overline{r_*})$ is shown by the dashed line. The spectra are shown by the contours which denote percentiles of all the distributions in each $r/\overline{r_*}$ class. The lightest colored contour therefore contains 95% of all the size distributions in each class.

3. SIZE DISTRIBUTIONS

Drizzle droplet size distributions measured with the PMS 2D-C probe (12.5-400 μm range) can be normalised well using an exponential mean radius $\overline{r_*}$ and total concentration N_{D*}. These are related to the $r > 20\mu$m concentration $N_{d,D}$ and radius $\overline{r_{d,D}}$ via

$$N_{D*} = N_{d,D} \exp(r_0/\overline{r_*}) \quad (1)$$

$$\overline{r_*} = \overline{r_{d,D}} - r_0 \quad (2)$$

where $r_0 = 20\mu$m is the defined threshold radius for drizzle drops. The exponential distribution is

$$dN/dr = (N_{D*}/\overline{r_*}) \exp(-r/\overline{r_*}). \quad (3)$$

which is shown together with the composite of 103 level-mean aircraft spectra in Fig. 4. This clearly shows that the level-mean drizzle droplet size distribution is well modelled as an exponential.

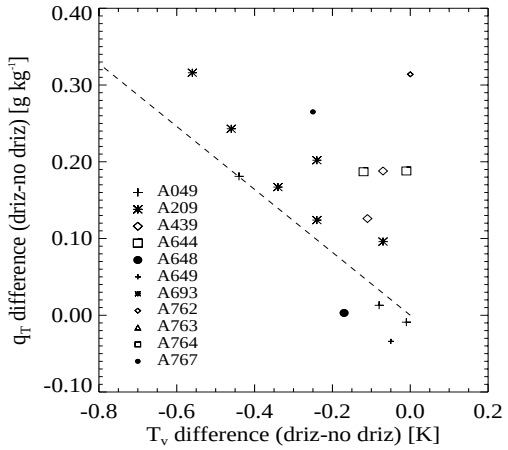

Figure 5: Difference between the mean subcloud virtual temperature (T_v, abscissa) and mean specific humidity (q_v, ordinate) in drizzle regions and drizzle-free regions for suitable subcloud runs. The dashed line corresponds to differences caused purely by evaporation.

4. MESOSCALE VARIABILITY

Evaporative cooling: To examine the hypothesis that evaporating drizzle droplets cool and moisten the subcloud layer, we conditionally sampled drizzle ($P > 0.01$ mm day^{-1}) and drizzle-free regions below cloud base. We calculated the difference in the virtual temperature and total water conent between the two regions (Fig. 5). There is a tendency for the drizzle containing regions to be slightly cooler and moister than the drizzle-free regions (see Jensen et al. 2000), but that temperature changes are less than would be expected from evaporation alone (dashed line).

Drizzle region sizes: Figure 6 shows the cumulative distribution of drizzle region size. We use 1km means taken on 60 km horizontal runs and define a value as a drizzle "patch" if it exceeds the median for that run. We then catalogue and size the regions. Around 50% are smaller than 2-3 km, with 90% smaller than 8 km. The largest cells ($> 15 - 20$ km) appear to be more prevalent in the subcloud layer, although these large patches are poorly sampled. Figure 7 shows a composite power spectrum of precipitation rate from the long runs - all the flights are included in this plot to reduce noise. There is a reasonably well-defined power law extending from the smallest scale (here 2km) to tens of km, suggesting that drizzle is a relatively scale invariant process at the small mesoscales. That the magnitude of the exponent is smaller than that for LWP (Davis et al. 1996) demonstrating that drizzle varies less smoothly in space than the liquid water path.

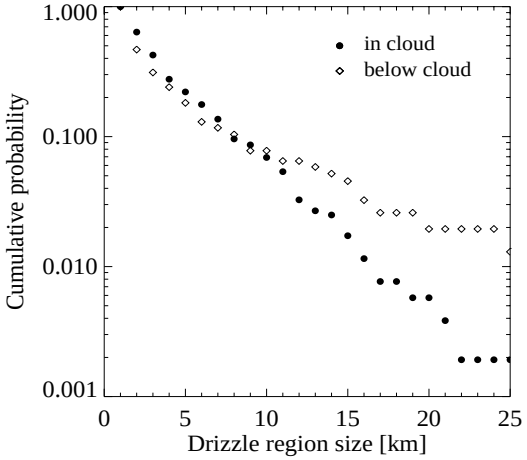

Figure 6: Cumulative distribution of drizzle cell sizes from all flights for in-cloud and below cloud runs. The ordinate shows the fraction of regions with sizes larger than shown on the abscissa.

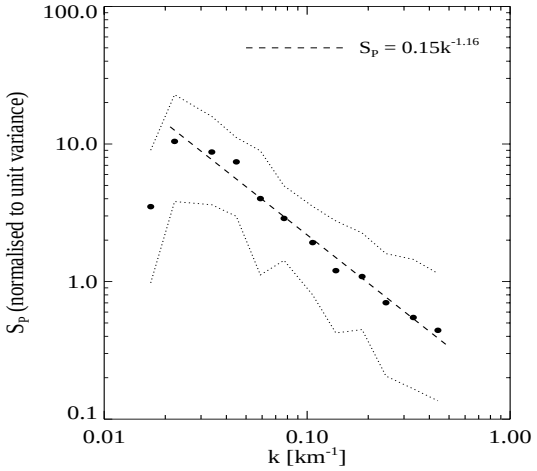

Figure 7: Composite normalised power spectrum of precipitation rate from all in-cloud and sub-cloud runs. The dotted lines show the 25th and 75th percentiles. The dashed line shows the best fit power law. Each contributing spectrum was first normalised with its variance before compositing.

We also used singular measures analysis to charac-

terize intermittency in precipitation rate, again using our 1 km dataset. Using the definition of intermittency used in Marshak et al. (1997) we find a mean intermittency parameter of $C_1 = 0.16 \pm 0.02$ for the entire dataset. The drizzle fields well described as being multifractal in nature (i.e. C_q is nonconstant). This indicates a considerably higher degree of intermittency compared with, for example, the cloud liquid water path in marine stratocumulus.

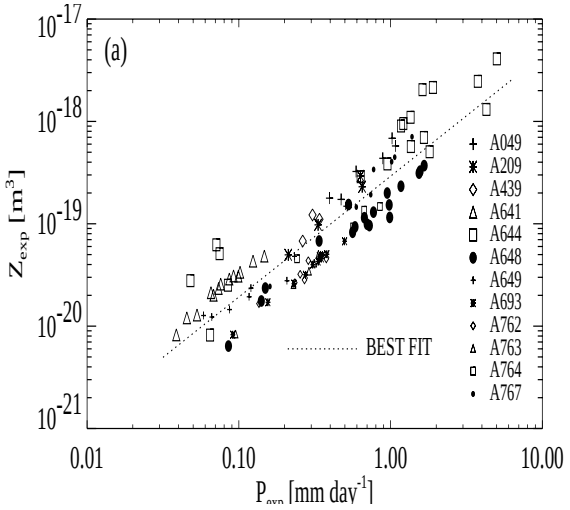

Figure 8: Derived reflectivities Z_{exp} plotted against precipitation rates P_{exp} for all the in-cloud extrapolated distributions. The dotted line represents the best fit power law.

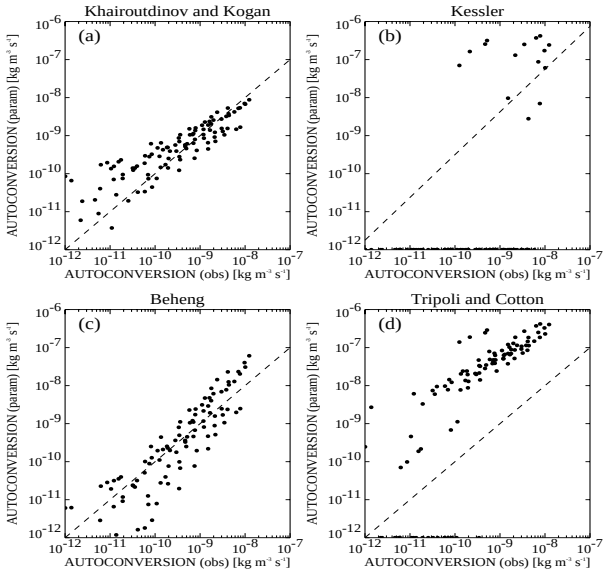

Figure 9: Comparison of autoconversion rates derived from the observed droplet size distributions (abscissae) and from the parameterizations of (a) Khairoutdinov and Kogan (2000); (b) Kessler (1960); (c) Beheng (1994); (d) Tripoli and Cotton (1980). Points for which the parameterized autoconversion rates are zero are shown along the abscissae.

5. Z-P RELATIONSHIPS

We show Z and precipitation rate P estimated from horizontally averaged size distributions for all flights in Fig. 8. There is a reasonably good relationship with a spread of approximately 3 in rainrate for a given Z. The best-fit relationship is $Z = 12.4P^{1.18}$ (Z in mm^6 m^{-3} and P in mm hr^{-1}), with $2-\sigma$ errors of approximately 50% in the constant and 0.11 in the exponent. We hope to compare this expression with similar rates derived during other campaign in marine stratocumulus.

6. VALIDATING DRIZZLE PARAMETERIZATIONS

We have also used the size distribution data to validate parameterizations commonly used to simulate precipitation in marine boundary layer cloud. Conversion of cloud droplets to drizzle droplets is often treated using an autoconversion rate which is parameterized using bulk parameters (liquid water content and cloud droplet concentration). We derive the autoconversion rate from the observed run-mean size distributions and compare with four parameterizations (Fig. 9). Interestingly, Tripoli and Cotton (1980), widely used in the GCM community, overpredicts the autoconversion rate by a factor of 1-2 *orders of magnitude*, whereas Khairoutdinov and Kogan's scheme works reasonably well. The Tripoli and Cotton overprediction is in accordance with the results of Baker (1993). Accretion rates from all these schemes are in much better agreement with observations (not shown).

I am grateful to the staff and aircrew at the Met Research Flight whose efforts were invaluable in obtaining this dataset.

REFERENCES

Baker, M. B., 1991: Variability in concentrations of cloud condensation nuclei in the marine cloud-topped boundary layer. *Tellus*, **45B**, 458-472.

Beheng, K. D., 1994: A parameterization of warm cloud microphysical conversion processes. *Atmos. Res.*, **33** 193-206.

Davis, A., A. Marshak, W. Wiscombe, R. Cahalan, 1996: Scale invariance of liquid water distributions in marine stratocumulus. Part I: Spectral properties and stationarity issues. *J. Atmos. Sci.*, **53**, 1538-1558.

Jensen, J. B., Lee, S., Krummel, P. B., Katzfey, J., Gogosa D., 2000: Precipitation in marine cumulus and stratocumulus. Part I: Thermodynamic and dynamic observations of closed cell circulations and cumulus bands. *Atmos. Res.*, **54**, 117-155.

Kessler, E., 1969: On the distribution and continuity of water substance in atmospheric circulations. *Meteor. Monogr.*, **32**, 84pp, American Meteorological Society.

Khairoutdinov, M. and Y. Kogan, 2000: A new cloud physics parameterization in a large-eddy simulation model of marine stratocumulus. *Mon. Wea. Rev.*, **128**, 229-243.

Marshak, A., A. Davis, W. Wiscombe, and R. Cahalan, 1997: Scale invariance in liquid water distributions in marine stratocumulus. Part II: Multifractal properties and intermittency issues. *J. Atmos. Sci.*, **54**, 1423-1444.

Nicholls, S., and J. Leighton, 1986: An observational study of the structure of stratiform cloud sheets: Part I. Structure *Quart. J. Roy. Meteorol. Soc.*, **112**, 431-460.

Tripoli, G. J. and W. R. Cotton, 1980: A numerical investigation of several factors contributing to the observed variable density of deep convection over South Florida *J. App. Meteorol.*, **19**, 1037-1063.